

A modeling study of a borehole radar system as a permanent down-hole sensor

Mattia Miorali*, Evert Slob, Delft University of Technology and Rob Arts, Delft University of Technology and TNO

SUMMARY

A technique capable of capturing the dynamics of reservoir fluids in the proximity of production wells would provide enormous benefits to the reservoir management. In fact, monitoring can be used to develop a feedback loop between measurements and control technologies to optimize production. This paper validates the feasibility of a borehole radar tool as a permanent down-hole sensor for near-wellbore imaging. We think that radar technology would be successful to prevent water encroachment in thin oil rims and to monitor steam chamber growth in Steam Assisted Gravity Drainage (SAGD) processes.

INTRODUCTION

A recent important innovation in the oil industry has been the application of measurement and control techniques to improve the oil recovery factor. In fact, a new generation of wells, called smart wells, allow to monitor well and reservoir conditions through down-hole sensors and to control the inflow of fluids from the reservoir to the well with remotely controllable valves. Figure 1 shows a schematic representation of a smart horizontal well (Jansen et al., 2008). The outer part of the well is divided in different compartments by rubber elements called packers. Each individual compartment of the well is equipped with inflow control valves (ICVs) that can control the flow from the compartments to the inner part of the well. Adjusting the setting of the ICVs in response to monitoring data obtained from down-hole sensors can significantly improve the oil production (Glandt, 2005). A typical application is the management of undesired fluids to prevent early breakthrough within the production wells. This is a big problem in any secondary or tertiary recovery phase method, where the injection of fluids like water or steam is necessary to maintain the reservoir pressure and/or to displace the oil from injection wells towards production wells. The sensors can see the arrival of undesired fluids and the valves can be set so that the steam or water fronts sweep the reservoir in the most effective way. Currently, the most used permanent down-hole sensors measure pressure and temperature but give a poor description of the fluid reservoir conditions outside the well. Therefore, there is an intense research effort to discover new monitoring techniques that could capture the fluid dynamics at larger distances from the well. In this paper we discuss the use of radar technology as a potential monitoring method. Given the characteristic of the EM wave propagation in the radar frequencies, the potential imaging capacity of a borehole radar tool is in the order of ten meters. This distance would fit the imaging necessity in Steam Assisted Gravity Drainage (SAGD) processes or in thin oil rim reservoirs. Figure 2 shows a potential application in a SAGD process. Source of inspiration for our research are the proved benefits of control strategies (Addiego-Guevara and Jackson,

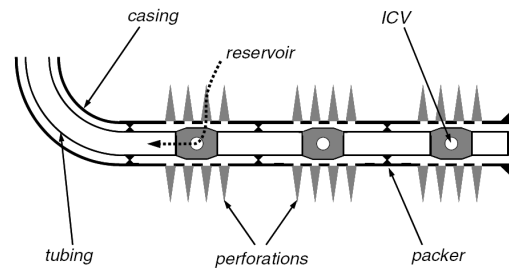


Figure 1: Schematic representation of a smart well. The perforations connect the reservoir to the annulus, the area between the casing and the tubing, which is divided in individual compartments by rubber elements called packers. Each compartment is equipped with ICVs and down-hole sensors.

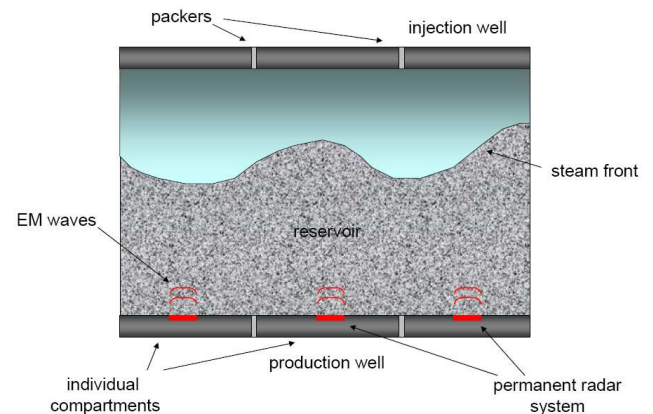


Figure 2: Schematic representation of a potential implementation of a radar system as a down-hole permanent sensor in a SAGD process. The steam injection is necessary to reduce the high viscosity of the heavy oil, which is then driven toward the production well by gravity.

2008) and previous work on the feasibility of borehole radar measurements as an imaging technique for oil field applications (Chen and Oristaglio, 2002).

ELECTROMAGNETIC WAVE PROPAGATION

The feasibility of a borehole radar tool as a permanent down-hole sensor mainly depends on the properties that describe the EM wave propagation, attenuation and phase distortion. Both these properties can be derived by the complex wavenumber $\gamma = \gamma_r + i\gamma_i$. The real component γ_r represents the attenuation part and the imaginary component γ_i represents the propagating part; these are respectively given by:

borehole radar system as a permanent down-hole sensor

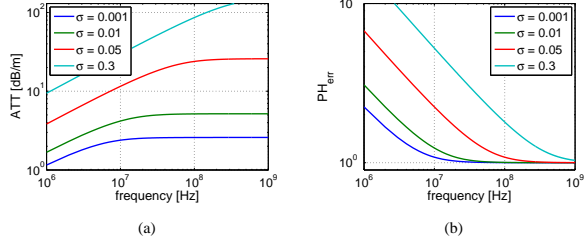


Figure 3: Wave attenuation ATT (fig. 3a) and phase distortion PH_{err} (fig. 3b) versus frequency for different values of conductivity σ and a fixed permittivity ($\epsilon_r = 10$)

$$\gamma_r = \frac{\omega}{c} \left[\frac{1}{2} \sqrt{1 + \delta^2} - \frac{1}{2} \right]^{1/2}, \quad (1)$$

$$\gamma_i = \frac{\omega}{c} \left[\frac{1}{2} \sqrt{1 + \delta^2} + \frac{1}{2} \right]^{1/2}, \quad (2)$$

where ω is the frequency, $c = (\epsilon\mu)^{-1/2}$, $\delta = \sigma/\omega\epsilon$ and $\mu = \mu_r\mu_0$, σ and $\epsilon = \epsilon_r\epsilon_0$ are the EM properties of a medium, respectively, magnetic permeability, electric conductivity and electric permittivity; μ_r is the relative permeability and ϵ_r is the relative permittivity, μ_0 and ϵ_0 are constant ($\mu_0 = 4\pi \times 10^{-7}$, $\epsilon_0 = 8.8542 \times 10^{-12}$). Values of the attenuation (ATT), in decibels, and of the phase distortion (PH_{err}) are given by the following equations:

$$ATT = 20 \log_{10}(e^{\gamma_r}), \quad (3)$$

$$PH_{err} = \frac{\gamma_i}{\omega\sqrt{\mu\epsilon}}. \quad (4)$$

PH_{err} is the ratio of the actual phase constant to its value in a non-conductive medium. We have considered realistic values of EM properties and we have studied their effect on ATT and PH_{err} . We have used the Complex Refractive Index Model (CRIM) model to get effective values of permittivity and Archie's law for effective values of conductivity, for geologic material the magnetic permeability is a constant, $\mu_r = 1$. CRIM is the most used model in the radar range of frequencies, since it is the one that better fits laboratory measurements (Roth et al., 1990; Seleznev et al., 2004). The natural regime for radar measurement is satisfied when $\delta \ll 1$, so that attenuation and phase distortion becomes independent of frequency and wave propagation prevail over diffusion phenomena. Analysis show that this requirement is answered for frequencies above 100 MHz and the main constrain is given by the conductivity (fig.3). Permittivity does not have a relevant impact. We found that the natural regime for EM propagation would be favorable in reservoirs with $\sigma < 0.03$ S/m.

The effect of the conductivity is clearer in the time domain. We use a Finite-Difference Time-Domain electromagnetic wave simulator, GPRMAX (Giannopoulos, 1997), to study how the propagation of a wavelet is affected by different values of σ . The EM source is given by a ricker excitation function. In figure 4 the time waveform and the amplitude spectra of the

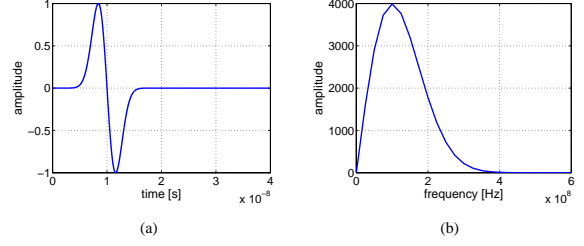


Figure 4: Time waveform (fig. 4a) and amplitude spectra (fig. 4b) of the ricker excitation function. The center frequency is 100 MHz.

ricker wavelet are shown. An increase of conductivity makes the detection of a signal more difficult; moreover, the consequent increase of phase distortion reduce the resolution of the wave and the ability to distinguish multiple reflections (fig. 5).

REFLECTIVITY OF AN INTERFACE

Another important parameter for the feasibility of a borehole radar system is the reflectivity of the interface to be detected, the steam or the water front. If the reflectivity of an interface is weak, a radar system may not be able to detect the reflection from the interface. The reflectivity expresses the amount of reflected energy and it depends on the reflection coefficient, which can be split into a transverse electric (TE) mode and into a transverse magnetic mode (TM). For a single planar interface, the reflection coefficients are given by:

$$r_{TE} = \frac{c_2 \sqrt{\cos^2 \theta - i\delta_1} - c_1 \sqrt{1 - c^2 \sin^2 \theta - i\delta_2}}{c_2 \sqrt{\cos^2 \theta - i\delta_1} + c_1 \sqrt{1 - c^2 \sin^2 \theta - i\delta_2}}, \quad (5)$$

$$r_{TM} = \frac{\eta_2 c_2 \sqrt{\cos^2 \theta - i\delta_1} - \eta_1 c_1 \sqrt{1 - c^2 \sin^2 \theta - i\delta_2}}{\eta_2 c_2 \sqrt{\cos^2 \theta - i\delta_1} + \eta_1 c_1 \sqrt{1 - c^2 \sin^2 \theta - i\delta_2}}, \quad (6)$$

where the subscript $i = 1, 2$ denotes two different media, θ denotes the angle of incidence, $\delta_i = \sigma_i/\omega\epsilon_i$, c_i is the velocity of the medium and $\eta_i = (\sigma_i + i\omega\epsilon_i)/(\sigma_i + i\omega\epsilon_i)$. Figure 6a shows the TE reflected energy $|r_{TE}|^2$ when a plane wave traveling in a relatively resistive medium ($\epsilon_{r1} = 10$ and $\sigma_1 = 0.01$ S/m) strikes an interface, which delimits a second medium with different EM properties at normal incidence. The permittivity contrast dominates the reflected energy when σ_2 is lower or in the same range of σ_1 ; when $\sigma_2 \gg \sigma_1$ the conductivity contrast plays the most important role and it causes a large increase of the reflected energy. Production wells are located in resistive medium and water or steam fronts delimit regions with a much higher permittivity and conductivity, therefore, this is the ideal condition to have strong reflections. The magnitude of the reflected energy depends on the polarization of the incident wave and the angle of incidence. In case of normal incidence, $|r_{TE}|^2$ is equal to $|r_{TM}|^2$, since both TE and TM waves are polarized parallel to the interface. As soon as

borehole radar system as a permanent down-hole sensor

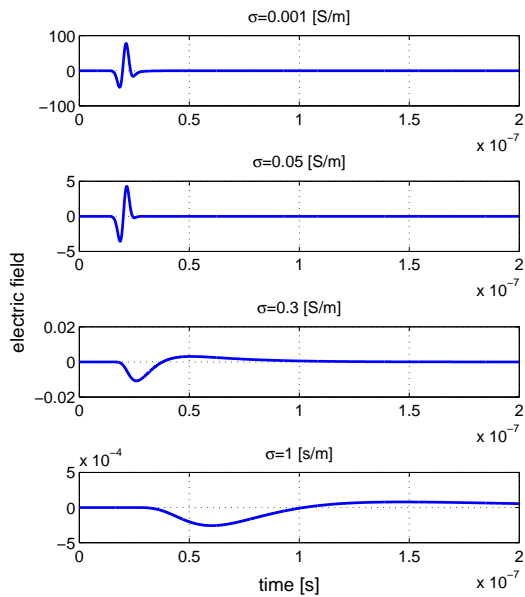


Figure 5: Electric field in the time domain for a 100 MHz ricker wavelet that travels the same distance (1 m) in a medium with a fixed permittivity ($\epsilon_r = 8$) and with different value of conductivity: $\sigma = 0.001$ S/m, $\sigma = 0.05$ S/m, $\sigma = 0.3$ S/m, $\sigma = 1$ S/m.

the angle of incidence θ is non zero, TE waves present a higher reflectivity, TM waves, instead, are less reflected, because they are polarized in the plane perpendicular to the interface and tend to be transmitted. Anyway, the difference between $|r_{TE}|^2$ and $|r_{TM}|^2$ is limited to the region where the permittivity contrast dominates. These considerations make TE wave measurements more powerful than TM measurements. We can also deduct that an array of sources and receivers would allow to exploit the higher reflected energy of oblique reflections. However, this benefit is decreased because of the stronger attenuation that would be generated by the longer travel path.

MODEL OF A SAGD PROCESS

We model different stages of a SAGD process with GPRMAX 2D. We define a typical heavy oil environment, where the oil is located in a sand layer that is embedded by layers of shale. In the upper region of the reservoir there is the injection well, used to inject steam. The steam reduces the high viscosity of the heavy oil and makes the oil drain toward the production well, located in the lower part of the reservoir. We give the material realistic EM properties (reservoir: $\epsilon_r = 8$, $\sigma = 0.01$ S/m; shale: $\epsilon_r = 14$, $\sigma = 0.01$ S/m; reservoir invaded by steam: $\epsilon_r = 8$, $\sigma = 0.01$ S/m; the wells are modeled as a PEC (Perfect Electric Conductor) medium). We locate an EM source in the upper part of the production well. The receiver is set at the same position of the source like in a monostatic radar system.

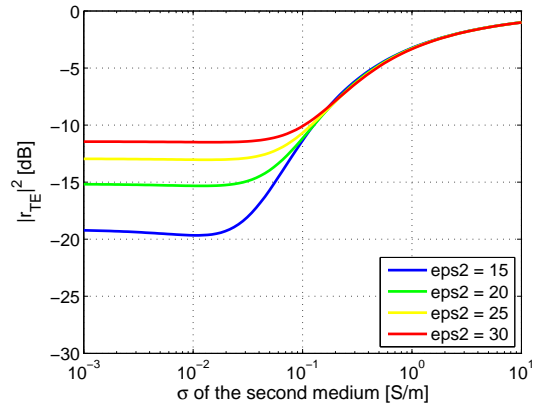


Figure 6: Reflectivity of a single planar interface with varying properties of medium 2 at 100 MHz for a normal incidence. Medium 1 has fixed properties: $\epsilon_r = 10$ and $\sigma = 0.01$ S/m.

The EM source is given by a ricker excitation function (fig. 4). The space domain is delimited by absorbing boundary conditions that do not introduce artificial reflections (Giannopoulos, 2008). We study the reflections for the initial conditions and for four sequent stages of a SAGD process, when the steam is respectively 4 m, 3 m, 2 m, and 1 m from the source. The steam is modeled as it spreads equally in all the direction, so such as a growing circle. To better understand the effect of the borehole on the EM responses, we investigate different configurations of the source. As first case, we locate the source on the boundary of the borehole. Then we set the source on the boundary of a high dielectric medium ($\epsilon_r = 25$, $\sigma = 0.001$ S/m) located above the borehole and we study the effect of the thickness of the dielectric medium on the EM responses. In figure 7 it is possible to see the model geometry for different stages of the SAGD process when the dielectric medium is used.

RESULTS

We show the results in a time-lapse way because we are studying changes over time. The response of the background condition is subtracted from the response of each following stages. In the case the source is on the boundary of the casing, no reflections are recorded. This is due to the fact that the metal acts as a perfect reflector and reverse the polarity of the wavelet, so that the signal is destroyed. If the source is moved upward the destructive interference is reduced but the source should be located too far from the borehole to get detectable signal and this is not feasible. In the case a high dielectric medium is located on the upper part of the borehole, the amplitude of the EM responses is strongly increased. Moreover, the thickness of the dielectric can be set so that there is a constructive interference between the emitted signal and the signal reflected by the casing of the borehole. An idea of the time delay necessary to get constructive interference can be deducted by the time waveform of the source function; for the source we use, it is around 4 ns. We show the EM responses recorded when a dielectric

borehole radar system as a permanent down-hole sensor

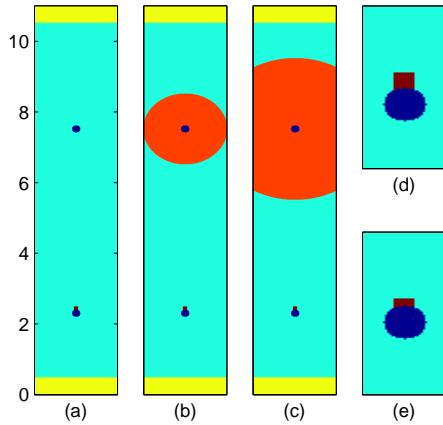


Figure 7: Model geometry for different stages of the SAGD process: background condition (fig. 7a) and steam, respectively, 4 m (fig. 7b) and 3 m (fig. 7c) from the source. The source is set at the upper boundary of a high dielectric medium located above the production well. A zoom in of a borehole equipped with a 10 cm and 5 cm dielectric medium is shown respectively in fig. 7d and fig. 7e

medium of 5 cm and 10 cm is used (fig. 8 and fig. 9). For the case of 10 cm the reflected amplitudes are higher because the interference is almost perfectly constructive. Without using any dielectric, responses of the same range can be obtained if the EM source is located 20 cm above the casing of the borehole.

CONCLUSIONS

This study suggests that a borehole radar system could be used as an imaging tool to probe the near-well region of several meters. This makes it especially suitable for application in thin oil rims or SAGD processes. Reflections generated by water/steam fronts are strong enough to be detected. The main constraint is the conductivity of the formation where the radar system is located; a high conductivity makes attenuation and phase distortion too high for wave propagation. We suggest that a high dielectric medium surrounding the production well could be used to increase the amplitude of the reflected signal.

ACKNOWLEDGMENTS

This research was carried out within the context of the IS-APP Knowledge Center. ISAPP - Integrated System Approach Petroleum Production - is a co-operation project of Shell International Exploration and Production BV, TU Delft, and Netherlands Organization for Applied Research TNO.

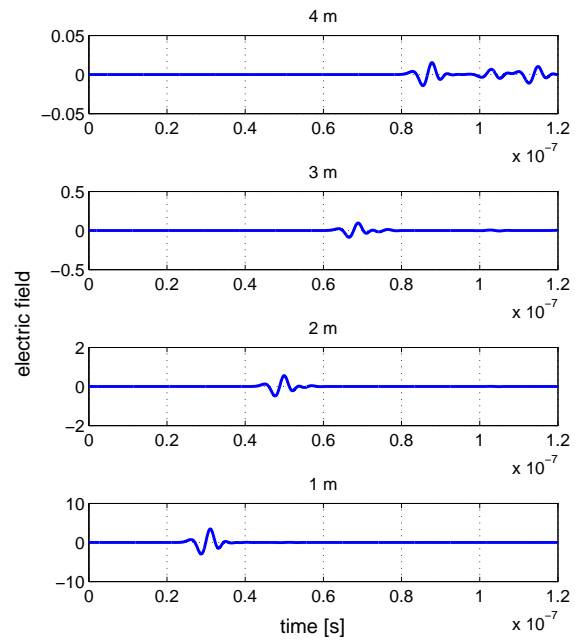


Figure 8: Time-lapse EM responses for four stages of a SAGD process when the borehole is equipped with a 5 cm dielectric medium.

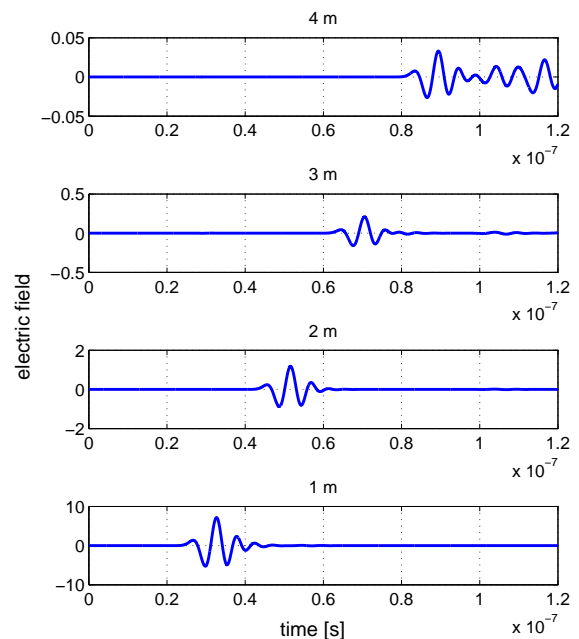


Figure 9: Time-lapse EM responses for four stages of a SAGD process when the borehole is equipped with a 10 cm dielectric medium.

borehole radar system as a permanent down-hole sensor

REFERENCES

- Addiego-Guevara, E. A. and M. D. Jackson, 2008, Insurance value of intelligent well technology against reservoir uncertainty: SPE, 1–16.
- Chen, Y. H. and M. L. Oristaglio, 2002, A modeling study of borehole radar for oil-field applications: Geophysics, **67**, 1486–1494.
- Giannopoulos, A., 1997, The investigation of transmission-line matrix and finite-difference time-domain methods for the forward problem of ground penetrating radar: PhD thesis, Department of Electronic, University of York, UK.
- , 2008, An improved new implementation of complex frequency shifted pml for the FDTD method: IEEE Transactions on Antennas and Propagation, **56**, 2995–3000.
- Glandt, C. A., 2005, Reservoir management employing smart wells: a review: SPE Drilling and Completion, **20**, 281–288.
- Jansen, J. D., O. H. Bosgra, and P. M. V. den Hof, 2008, Model-based control of multiphase flow in subsurface oil reservoirs: Journal of Process Control, **18**, 846–855.
- Roth, K., H. Schulin, H. Fluhler, and W. Attinger, 1990, Calibration of time domain reflectometry for water content measurements using a composite dielectric approach: Water Resources Research, **26**.
- Seleznev, N. V., A. Body, T. Habashy, and S. Luthi, 2004, Dielectric mixing laws for partially saturated carbonate rocks: 45th Annual Logging SPWLA Symposium.